

Sequential change-point detection for mutually exciting point processes over networks

Haoyun Wang^a, Liyan Xie^a, Yao Xie^a, Alex Cuozzo^b, Simon Mak^b

^aSchool of Industrial and Systems Engineering, Georgia Institute of Technology, Atlanta, Georgia, USA,

^aDepartment of Statistical Science, Duke University, Durham, North Carolina, USA

Abstract

We present a new CUSUM procedure for sequentially detecting change-point in the self and mutual exciting processes, a.k.a. Hawkes networks using discrete events data. Hawkes networks have become a popular model for statistics and machine learning due to their capability in modeling irregularly observed data where the timing between events carries a lot of information. The problem of detecting abrupt changes in Hawkes networks arises from various applications, including neuronal imaging, sensor network and social network monitoring. Despite this, there has not been a computationally and memory-efficient online algorithm for detecting such changes from sequential data. We present an efficient online recursive implementation of the CUSUM statistic for Hawkes processes, both decentralized and memory-efficient, and establish the theoretical properties of this new CUSUM procedure. We then show that the proposed CUSUM method achieves better performance than existing methods, including the Shewhart procedure based on count data, the generalized likelihood ratio (GLR) in the existing literature, and the standard score statistic. We demonstrate this via a simulated example and an application to population code change-detection in neuronal networks.

Keywords: Change-point detection; CUSUM procedures; Hawkes process; Online algorithm.

1 Introduction

Point processes are widely used for modeling the so-called discrete events data, which consists of a series events times and associated additional information. Recently, a class of mutual

Address correspondence to Yao Xie, School of Industrial and Systems Engineering, Georgia Institute of Technology, Atlanta, Georgia, 30332, USA; E-mail: yao.xie@isye.gatech.edu

exciting point processes, known as Hawkes process (Hawkes, 1971), has gained much popularity in the statistics and machine learning literature. Hawkes processes provide a flexible model for capturing spatio-temporal correlations, and have been successfully applied in a wide range of domains including seismology (Ogata, 1988, 1998), criminology (Mohler et al., 2011), epidemiology (Rizoiu et al., 2018), social networks (Yang and Zha, 2013), finance (Hawkes, 2018), and neural activity (Reynaud-Bouret et al., 2013).

Detection of abrupt changes in the Hawkes process is a fundamental problem, which aims to detect the change as quickly as possible subject to false alarm constraints. For instance, in sensor network monitoring, we would like to detect any changes as soon as possible using a stream of event data; such change may represent a shift in the systems status or event anomalies. The challenges for detecting changes in Hawkes processes include handling complex spatial and temporal dependence of the event data streaming and long-term dependency; we need to develop computationally efficient online algorithms with performance guarantees.

A motivating application for our study is neuronal network analysis, where we are interested in inferring the network connectivity and detecting neural state changes from experimental data – the neural spike train data, which records the sequence of times when a neuron fires an action potential. Hawkes processes provide an intuitive modeling framework for such data: its mutually exciting property naturally mimics neuron-to-neuron influence’s electrochemical dynamics. The model’s probabilistic nature can capture noisy influences on the network (due to unobserved neurons or external stimuli). There has been much work on applying Hawkes models for a range of neuroscience problems, e.g., functional connectivity (Lambert et al., 2018) and uncertainty quantification (Wang et al., 2020b). The problem of change-point detection is fundamental for neuronal network analysis, allowing researchers to identify when an external stimulus is internalized. These change-points often arise from sparse population code changes in the biological network (Tang et al., 2018). Sparse population coding provides a sparse and distributed representation of information over the biological network, with each neuron representing the presence (or absence) of a specific feature. Figure 1 illustrates this idea. Here, each dot represents a neuron in the visual cortex. Colored dots show neurons that respond to seeing a cat or a dog, and shared dots represent common features between both animals (e.g., mammal, pet). Identifying the change-point between two population codes allows scientists to investigate the relationship between stimulus and response timing and better understand each neuron’s role in the population code.

While there has been much study for estimating Hawkes processes in the literature (see Reinhart (2018) for a recent survey), change-point detection for Hawkes processes is much less studied. In Wang et al. (2020a), the offline change-point detection for high-dimensional

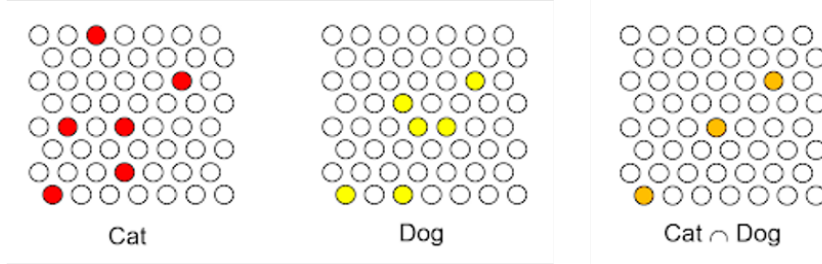


Figure 1: Visualizing sparse population coding for neuronal networks. Each dot represents a neuron, and colored dots show neurons which respond to seeing a cat or a dog.

Hawkes processes was studied, and the goal is to estimate the (multiple) change-points. In [Rambaldi et al. \(2018\)](#), a model selection scheme was proposed to identify the presence of exogenous events that increase the intensity of the Hawkes process for a given time period. A cumulant based multi-resolution segmentation algorithm was proposed in [Zhou et al. \(2020\)](#) to find the optimal partition of the nonstationary Hawkes process into several non-overlapping segments. On the contrary, we focus on sequential detection to detect the change as quickly as possible. Online change-point detection for Hawkes process was considered in [Li et al. \(2017\)](#), where the generalized likelihood ratio test was used to detect the change with unknown post-change parameters. The expectation-maximization (EM) algorithm was used in [Li et al. \(2017\)](#) to estimate the unknown post-change parameter, and there is no recursive implementation.

In this paper, we present a new CUSUM procedure for sequential change detection in Hawkes processes. The new CUSUM procedure is computationally efficient and memory-efficient as a recursive procedure, which is crucial for its online implementation. We present the theoretical properties of the CUSUM procedure. We also compare the detection procedures with existing change detection algorithms based on the generalized likelihood ratio statistic ([Li et al., 2017](#)) and a score statistic using numerical examples. Finally, we consider a real-world application of detecting neuronal network population code change. The results show that the CUSUM procedure outperforms the alternative methods.

The rest of the paper is organized as follows. Section 2 introduces the basics for the Hawkes process. Section 3 sets up the change-point detection problem. Section 4 presents the proposed CUSUM procedure and its theoretical properties. Section 5 discusses some alternative detection methods. Section 6 numerically compares their performance. Section 7 demonstrates a real-world application using neural spike train data. Section 8 concludes the paper with some discussions.

2 Preliminaries

A temporal point process is a random process whose realization consists of a sequence of discrete events occurring at times $\{t_i, i = 1, 2, \dots\}$, with $t_i \in \mathbb{R}^+$. Let the history \mathcal{H}_{t^-} be the sequence of times of events $\{t_1, t_2, \dots, t_n\}$ up to but *not* including time t . Strictly speaking, \mathcal{H}_{t^-} is a filtration, that is, an increasing sequence of σ -algebras. Let N_t represents the number of events before time t , then N_t is a counting process which can be defined as:

$$dN_t = \sum_{t_i \in \mathcal{H}_t} \delta(t - t_i) dt, \quad (2.1)$$

where δ is the Dirac function. The sequence of discrete event times $\{t_i, i = 1, 2, \dots\}$ can be regarded as when the counting process N_t has jumped.

A point process can be characterized by conditional intensity function, denoted as $\lambda(t)$. Originally conditional intensity function is also called hazard function (Rasmussen, 2011) and is defined as

$$\lambda(t) = \frac{f^*(t)}{1 - F^*(t)}, \quad (2.2)$$

where $f^*(t)$ is the probability density function of the next event time conditional on the past, and $F^*(t)$ is the associated conditional cumulative distribution function capturing the probability of the $(n + 1)$ -th event happening before time t :

$$F^*(t) = \mathbb{P}\{t_{n+1} < t | \mathcal{H}_{t^-}\}.$$

Thus if we consider a small time interval $[t, t + dt]$, we have

$$\lambda(t)dt = \frac{f^*(t)dt}{1 - F^*(t)} = \frac{\mathbb{P}(t_{n+1} \in [t, t + dt])}{\mathbb{P}(t_{n+1} \geq t)} = \mathbb{P}\{t_{n+1} \in [t, t + dt] | \mathcal{H}_{t^-}\}.$$

2.1 One-Dimensional Point Processes

For one-dimensional Hawkes process, the intensity function takes the form (Hawkes, 1971):

$$\lambda(t) = \mu(t) + \alpha \int_0^t \varphi(t - \tau) dN_\tau, \quad (2.3)$$

where $\mu(t)$ is the base intensity, α is the influence parameter, and $\varphi(t)$ is a normalized kernel function satisfying $\int \varphi(t)dt = 1$. A commonly used kernel function is the exponential kernel $\varphi(t) = \beta e^{-\beta t}$ with $\beta > 0$. We assume $0 \leq \alpha < 1$ to ensure a stationary process.

Given event times $\{t_1, t_2, \dots, t_n\}$ which happened before a given time $t < \infty$, the log-

likelihood function for the Hawkes process can be written as follows (see [Daley and Vere-Jones \(2003\)](#) for details):

$$\ell_t = \sum_{i=1}^n \log \left[\mu(t_i) + \alpha \sum_{t_j < t_i} \varphi(t_i - t_j) \right] - \int_0^t \mu(s) ds - \alpha \sum_{i=1}^n \int_{t_i}^t \varphi(s - t_i) ds. \quad (2.4)$$

In case of the exponential kernel $\varphi(t) = \beta e^{-\beta t}$ and a constant base intensity μ , (2.4) reads

$$\ell_t = \sum_{i=1}^n \log \left[\mu + \alpha \sum_{t_j < t_i} \beta e^{-\beta(t_i - t_j)} \right] - \mu t - \alpha \sum_{i=1}^n [1 - e^{-\beta(t - t_i)}]. \quad (2.5)$$

As we will see in the following, the log-likelihood plays a key role in sequential change detection procedures.

2.2 Network Point Processes

The multivariate Hawkes process on a network with D nodes is represented by a series of event times together with their location $\{(t_i, u_i), i = 1, 2, \dots\}$, where $t_i \in \mathbb{R}^+$ is the event time and $u_i \in [D]$ is the node on which the i -th event occurs. Here we use $[D]$ to represent the set $\{1, \dots, D\}$. The intensity function for node i at time t is

$$\lambda_i(t) = \mu_i(t) + \sum_{j \in [D]} \alpha_{ij} \int_0^t \varphi_{ij}(t - s) dN_s^j,$$

where $\mu_i(t)$ is the base intensity at node i , α_{ij} is the influence parameter from node j to node i , $\varphi_{ij}(t)$ is a normalized kernel function, and N_t^j is a counting process on node j :

$$dN_t^j = \sum_{k: t_k < t, u_k = j} \delta(t - t_k) dt.$$

The log-likelihood function for the network setting up to time t is given by:

$$\ell_t(A) = - \sum_{i \in [D]} \int_0^t \lambda_i(s) ds + \sum_{i \in [D]} \int_0^t \log(\lambda_i(s)) dN_s^i, \quad (2.6)$$

where $A = (\alpha_{ij})_{i,j \in [D]} \in \mathbb{R}^{D \times D}$ is the matrix representation for the influence parameters.

Remark 2.1. Note that the likelihood function decouples as the summation over D nodes: it consists of the sum of the log-likelihood at each node. The intensity function $\lambda_i(\cdot)$ only involves events observed on the neighbors of i (i.e., the nodes that will influence node i).

This property may enable us to develop distributed change-point detection procedure, i.e., the nodes can compute their likelihood in parallel and only need to communicate with their neighbors (if the neighborhood information is known).

3 Problem Set-up

The problem of change-point detection for Hawkes networks sets up as follows. Assume there may exist a true change-point time $\kappa > 0$, and the event data follows one point process before the change-point and follows another point process afterward. We are particularly interested in two special cases: (i) The null point process is a Poisson process, whereas the alternative point process is a Hawkes point process; (ii) The null point process is a Hawkes point process, whereas the alternative point process is a different Hawkes point process, e.g., the influence parameter A has been shifted. Note that the first scenario can be seen as a specific case since the Poisson process can be treated as a special Hawkes process with influence parameters setting to be 0.

Consider the hypothesis test to detect the temporal pattern shifts in the Hawkes process, assuming the Hawkes process is stationary and the change-point κ is an *unknown* variable, as follows:

$$\begin{aligned} H_0 : \quad & \lambda_i^*(s) = \mu_i(s) + \sum_{j \in [D]} \alpha_{ij,0} \int_0^s \varphi_{ij}(s-v) dN_v^j; \quad i \in [D], s \geq 0, \\ H_1 : \quad & \lambda_i^*(s) = \mu_i(s) + \sum_{j \in [D]} \alpha_{ij,0} \int_0^s \varphi_{ij}(s-v) dN_v^j; \quad i \in [D], 0 \leq s \leq \kappa, \\ & \lambda_i^*(s) = \mu_i(s) + \sum_{j \in [D]} \alpha_{ij,1} \int_\kappa^s \varphi_{ij}(s-v) dN_v^j; \quad i \in [D], s > \kappa, \end{aligned} \quad (3.1)$$

where $\lambda_i^*(s)$ denotes the true intensity for node i at time s . The pre-change parameter $\{\alpha_{ij,0}\}_{i,j \in [D]}$ is usually given from our knowledge of the process or can be estimated from reference data. The post-change parameter $\{\alpha_{ij,1}\}_{i,j \in [D]}$ is known in some scenarios, but more often it corresponds to an unexpected anomaly and we may not have enough data to estimate it in advance. Alternatively, we can treat the post-change parameters as the targeted smallest change to be detected.

A change detection procedure resolves the two hypothesis using a stopping time T , which is a function of the event sequence as we will explain in the next section.

4 CUSUM Detection Procedure

In this section, we present the cumulative sum (CUSUM) statistics based on the log-likelihood ratio. The CUSUM procedure was first proposed in [Page \(1954\)](#), assuming both the pre-

and post-change parameters. It is computationally efficient but less robust to parameter uncertainties (to make it more robust, we can use adaptive-CUSUM procedure such as that in [Xie et al. \(2020\)](#)). The CUSUM procedure is most commonly defined for i.i.d. observations, and recently there has also been much development in CUSUM for non i.i.d. observations ([Tartakovsky et al., 2014](#); [Xie et al., 2021](#)).

We first define the log-likelihood ratio function that will be used as the main building block. For a hypothesized change-point τ , the log-likelihood ratio of the model (3.1) up to time t can be derived as:

$$\ell_{t,\tau} = \sum_{i \in [D]} \int_{\tau}^t \log \left(\frac{\lambda_{i,\tau}(s)}{\lambda_{i,\infty}(s)} \right) dN_s^i - \sum_{i \in [D]} \int_{\tau}^t (\lambda_{i,\tau}(s) - \lambda_{i,\infty}(s)) ds, \quad (4.1)$$

where

$$\lambda_{i,\tau}(t) = \begin{cases} \mu_i(t) + \sum_{j \in [D]} \alpha_{ij,1} \int_{\tau}^t \varphi_{ij}(t-s) dN_s^j, & t > \tau, \\ \lambda_{i,\infty}(t), & 0 \leq t \leq \tau, \end{cases}$$

is the intensity for node i if the change-point happens at τ , and

$$\lambda_{i,\infty}(t) = \mu_i(t) + \sum_{j \in [D]} \alpha_{ij,0} \int_0^t \varphi_{ij}(t-s) dN_s^j,$$

is the intensity under the null hypothesis, where we use ∞ to indicate that the change never happens.

4.1 CUSUM Statistic

Given assumed post-change parameters, $\{\alpha_{ij,1}\}_{i,j \in [D]}$, the stopping time for CUSUM is given by

$$T_C = \inf\{t : \sup_{\tau < t} \ell_{t,\tau} > b\}, \quad (4.2)$$

where $\ell_{t,\tau}$ is the log-likelihood ratio statistic defined in (4.1), and $b > 0$ is a pre-specified threshold. The procedure stops when the log-likelihood ratio from some hypothesized change-point τ exceeds threshold b .

In contrast to the original CUSUM procedure ([Page, 1954](#)) where the samples are taken in a discrete-time fashion, here the CUSUM statistic is continuous-time and has memory. In particular, due to the memory of the process, the observations are *non-i.i.d.* and have complex dependence to the past. Therefore, we do not have a simple recursion as the vanilla version of the CUSUM procedure.

Next we derive an computationally efficient recursive algorithm for computing the CUSUM statistic for the network Hawkes process. We start with a lemma for the log-likelihood ratio $\ell_{t,\tau}$ which shows that, although the supremum of the log-likelihood ratio statistic over the unknown change-point appears to be on a continuum, it will be obtained at the observed event times.

Lemma 4.1. *Given the event times $\{t_i, i = 1, 2, \dots\}$, for any fixed t and k , $t > t_k$, there is*

$$\sup_{t_k < \tau \leq \min\{t_{k+1}, t\}} \ell_{t,\tau} = \lim_{\tau \rightarrow t_k^+} \ell_{t,\tau} =: \ell_{t,t_k^+},$$

and

$$\sup_{0 \leq \tau \leq t_1} \ell_{t,\tau} = \ell_{t,0}.$$

Lemma 4.1 says that we only need to consider the values of the log-likelihood evaluated as the past event times rather than a continuum of possible values for τ ; this will greatly simplify the computation of the log-likelihood ratio statistic.

Proof. For fixed event and any $\tau \in (t_k, \min\{t_{k+1}, t\}]$, the intensity $\lambda_{i,\tau}(s)$ at any time $s \geq \tau$ is a constant that does not depend on τ , and the first part of the log-likelihood ratio (4.1),

$$\sum_{i \in [D]} \int_{\tau}^t \log \left(\frac{\lambda_{i,\tau}(s)}{\lambda_{i,\infty}(s)} \right) dN_s^i,$$

is also a constant. For the second part,

$$- \sum_{i \in [D]} \int_{\tau}^t (\lambda_{i,\tau}(s) - \lambda_{i,\infty}(s)) ds,$$

the integrand is no larger than 0 because $\lambda_{i,\tau}(s) = \mu_i(s) \leq \lambda_{i,\infty}(s)$ for any $\tau < s \leq t_{k+1}$. Therefore the supremum of $\ell_{t,\tau}$ is reached when $\tau \rightarrow t_k^+$, which is

$$\sup_{t_k < \tau \leq \min\{t_{k+1}, t\}} \ell_{t,\tau} = \ell_{t,t_k^+}.$$

For the supremum w.r.t. τ over $[0, t_1]$, the equality can be derived using similar arguments. \square

For practical reasons such as computational efficiency, we can simplify the calculation in (4.2) which involves $\sup_{\tau < t} \ell_{t,\tau}$, by considering t on a discretized grid with a pre-specified grid size $\gamma > 0$, i.e., we only need to calculate the detection statistic $\sup_{\tau < n\gamma} \ell_{n\gamma,\tau}$ for $n \in \mathbb{Z}$.

Finally, with the discretization for both τ and t , the log-likelihood ratio $\ell_{n\gamma, t_k^+}$ and $\ell_{(n+1)\gamma, t_k^+}$ has the following relationship, given $n\gamma \geq t_k$,

$$\ell_{(n+1)\gamma, t_k^+} = \ell_{n\gamma, t_k^+} + \sum_{i \in [D]} \int_{n\gamma}^{(n+1)\gamma} \log \left(\frac{\lambda_{i, t_k^+}(s)}{\lambda_{i, \infty}(s)} \right) dN_s^i - \sum_{i \in [D]} \int_{n\gamma}^{(n+1)\gamma} (\lambda_{i, t_k^+}(s) - \lambda_{i, \infty}(s)) ds. \quad (4.3)$$

If we have access to the cumulative kernels

$$\Phi_{ij}(t) = \begin{cases} \int_0^t \varphi_{ij}(s) ds, & t \geq 0, \\ 0, & t < 0, \end{cases}$$

the recursion can be computed without numerical integration:

$$\begin{aligned} \ell_{(n+1)\gamma, t_k^+} &= \ell_{n\gamma, t_k^+} + \sum_{i \in [D]} \int_{n\gamma}^{(n+1)\gamma} \log \left(\frac{\lambda_{i, t_k^+}(s)}{\lambda_{i, \infty}(s)} \right) dN_s^i \\ &+ \sum_{i, j \in [D]} \int_0^{(n+1)\gamma} \alpha_{ij, 0} (\Phi_{ij}((n+1)\gamma - s) - \Phi_{ij}(n\gamma - s)) dN_s^j \\ &- \sum_{i, j \in [D]} \int_{t_k^+}^{(n+1)\gamma} \alpha_{ij, 1} (\Phi_{ij}((n+1)\gamma - s) - \Phi_{ij}(n\gamma - s)) dN_s^j. \end{aligned} \quad (4.4)$$

The CUSUM algorithm is summarized in Algorithm 1.

Remark 4.1 (Choice of grid size γ). The grid size γ corresponds to the updating frequency of the CUSUM statistics and is an important parameter to the CUSUM algorithm. There is a trade-off in choosing the parameter γ : a large γ might result in a larger detection delay, while a very small γ might lead to unnecessary computational complexity. It would be interesting to develop a method to choose γ adaptively.

4.2 Memory-Efficient CUSUM

The exact CUSUM algorithm requires remembering the entire history of events because all the past events influence the intensity function. In practice, we choose to neglect those events that happened a while ago to save memory, assuming that their influence on the present and the future is small, while achieving a similar performance.

Algorithm 1: CUSUM for Hawkes

Input: event times $\{(t_i, u_i), i = 1, 2, \dots\}$; pre-change parameters $\{\alpha_{ij,0}\}_{i,j \in [D]}$;
post-change parameters $\{\alpha_{ij,1}\}_{i,j \in [D]}$; **threshold** b ; **grid size** γ ;
Initialization: $n = 0, S_0 = 0, \ell_{0,0} = 0$;
while $S_{n\gamma} < b$ **do**
 $n := n + 1$;
 for $\tau \in \{t_k^+ : t_k < n\gamma\} \cup \{0\}$ **do**
 if $\tau < (n-1)\gamma$ **then**
 | calculate $\ell_{n\gamma,\tau}$ using (4.3) or (4.4);
 else
 | calculate $\ell_{n\gamma,\tau}$ using (4.1);
 end
 end
 $S_{n\gamma} := \max_{\tau} \ell_{n\gamma,\tau}$;
 if $S_{n\gamma} > b$ **then**
 | **Output** $T_c := n\gamma, \hat{\tau} := \arg \max_{\tau} \ell_{n\gamma,\tau}$;
 end
end

Consider the following *truncated kernel* with a width $B > 0$:

$$\tilde{\varphi}_{ij}(t) = \begin{cases} \varphi_{ij}(t), & t \leq B, \\ 0, & t > B. \end{cases}$$

Under the truncated kernel, an event has no influence over the whole process after B into the future, and we only need to keep events during $[t - B, t]$ in our memory for computation. With the truncated kernel $\tilde{\varphi}_{ij}$, the intensity for node i can be approximated by

$$\tilde{\lambda}_{i,\tau}(t) = \begin{cases} \mu_i(t) + \sum_{j \in [D]} \alpha_{ij,1} \int_{t-B}^t \varphi_{ij}(t-s) dN_s^j, & \tau < t - B, \\ \mu_i(t) + \sum_{j \in [D]} \alpha_{ij,1} \int_{\tau}^t \varphi_{ij}(t-s) dN_s^j, & t - B \leq \tau \leq t, \\ \mu_i(t) + \sum_{j \in [D]} \alpha_{ij,0} \int_{t-B}^t \varphi_{ij}(t-s) dN_s^j, & \tau > t. \end{cases} \quad (4.5)$$

Here for all $\tau \geq 0$, $\tilde{\lambda}_{i,\tau}(t)$ only depends on event data during $[t - B, t]$. Moreover, the intensity for $\tau < t - B$ does not depend on τ , which enables us to update the log-likelihood ratio recursively for small τ . If we also have access to the cumulative kernels $\Phi_{ij}, i, j \in [D]$,

the recursion step in (4.4) can be approximated by

$$\begin{aligned}
\ell_{(n+1)\gamma, t_k^+} &= \ell_{n\gamma, t_k^+} + \sum_{i \in [D]} \int_{n\gamma}^{(n+1)\gamma} \log \left(\frac{\tilde{\lambda}_{i, t_k^+}(s)}{\tilde{\lambda}_{i, \infty}(s)} \right) dN_s^i \\
&+ \sum_{i, j \in [D]} \int_{n\gamma - B}^{(n+1)\gamma} \alpha_{ij, 0} (\tilde{\Phi}_{ij}((n+1)\gamma - s) - \tilde{\Phi}_{ij}(n\gamma - s)) dN_s^j \\
&- \sum_{i, j \in [D]} \int_{\max\{t_k^+, n\gamma - B\}}^{(n+1)\gamma} \alpha_{ij, 1} (\tilde{\Phi}_{ij}((n+1)\gamma - s) - \tilde{\Phi}_{ij}(n\gamma - s)) dN_s^j, \quad (4.6)
\end{aligned}$$

where $\tilde{\Phi}_{ij}(t) = \Phi_{ij}(\min\{t, B\})$, and the summation is taken only for event times during $[n\gamma - B, (n+1)\gamma]$. The resulted CUSUM procedure is summarized in Algorithm 2.

Algorithm 2: Memory-efficient CUSUM for Hawkes

Input: event times $\{(t_i, u_i), i = 1, 2, \dots\}$; pre-change parameters $\{\alpha_{ij, 0}\}_{i, j \in [D]}$;
 post-change parameters $\{\alpha_{ij, 1}\}_{i, j \in [D]}$; threshold b ; grid size γ ;
Initialization: $n = 0, S_0 = 0, \ell_{0,0} = 0, \hat{\tau} = 0$;
while $S_{n\gamma} < b$ **do**

$n := n + 1$;
for $\tau \in \{t_k^+ : (n-1)\gamma \leq t_k < n\gamma\}$ **do**
 | calculate $\ell_{n\gamma, \tau}$ using (4.1) with (4.5);
end
for $\tau \in \{t_k^+ : (n-1)\gamma - B \leq t_k < (n-1)\gamma\}$ **do**
 | calculate $\ell_{n\gamma, \tau}$ using (4.3) with (4.5) or (4.6);
end
for $\tau \in \{t_k^+ : (n-2)\gamma - B \leq t_k < (n-1)\gamma - B\}$ **do**
 | **if** $\ell_{(n-1)\gamma, \tau} > \ell_{(n-1)\gamma, \hat{\tau}}$ **then**
 | | $\hat{\tau} := \tau$;
 | **end**
end
update $\ell_{n\gamma, \hat{\tau}}$ **from** $\ell_{(n-1)\gamma, \hat{\tau}}$ **using** (4.3) **with** (4.5) **or** (4.6);
 $S_{n\gamma} = \max_{\tau} \ell_{n\gamma, \tau}$;
if $S_{n\gamma} > b$ **then**
 | **Output** $T_C := n\gamma, \hat{\tau} := \arg \max_{\tau} \ell_{n\gamma, \tau}$;
end
end

We illustrate the effect of the truncation width B using a numerical example. The model is described in Section 6, where the kernel functions are all exponential:

$$\varphi_{ij}(t) = \beta e^{-\beta t}, t \geq 0, \quad \forall i, j \in [D]$$

with $\beta = 1$. Figure 2 shows the comparison between CUSUM statistics with and without kernel truncation. Both statistics with truncated kernel have the same trend with the exact CUSUM. When $B = 1/\beta$, 63.2% of the cumulative influence is preserved, and the statistic deviates from the exact CUSUM, which may result in a false alarm. When $B = 2/\beta$ preserving 86.5% of the cumulative influence, there is little difference between the two statistics.

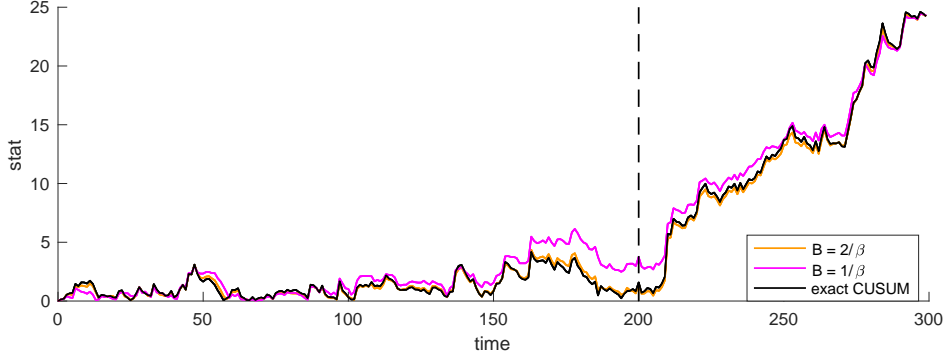


Figure 2: Comparison between CUSUM statistics with different truncation level B . The change happens at 200.

4.3 Theoretical Properties of CUSUM

In this section, we study the theoretical properties of CUSUM (as presented in Algorithm 1). The analysis helps us determine the proper threshold for the detection algorithm without using the Monte Carlo method, which is computationally expensive and prohibitive for some practical problems.

Two widely used performance metrics for sequential change-point detection are: (i) Average run length (ARL), defined as the expected value of the stopping time when there is no change, i.e., $\mathbb{E}_\infty[T]$, where \mathbb{P}_∞ is the probability measure on the sequence of event times when the change never occurs, and \mathbb{E}_∞ is the corresponding expectation; (ii) Expected detection delay (EDD), defined as the expected delay between the stopping time and the true change-point. Two common definitions for EDD can be found in [Lorden \(1971\)](#) and [Pollak \(1985\)](#), both of them consider the worst-case delay over all possible change-point values. In particular, if the true change-point is κ , then the EDD can be defined as $\mathbb{E}_\kappa[T - \kappa | T > \kappa]$, where \mathbb{P}_κ denotes the probability measure on the observations when the change occurs at time κ , and \mathbb{E}_κ denotes the corresponding expectation.

We establish a lower bound for ARL regarding the threshold b . Typically for the i.i.d. observation setting, the ARL grows exponentially with respect to the threshold b . Here although Hawkes process is a continuous time procedure, it is naturally discretized by the

event times; interesting, we obtain a similar result for the ARL of our CUSUM procedure:

Theorem 4.1 (ARL of CUSUM). *In Algorithm 1 under H_0 , the number of events happened before T_C satisfies*

$$\mathbb{E}_\infty [|\{k : t_k \leq T_C\}|] \geq \mathbb{E}_\infty [|\{k : t_k \leq \hat{\tau}\}|] \geq \left(\frac{1 - o(1)}{2} \right) e^b.$$

Proof. For each fixed τ , $(\exp \ell_{t,\tau})_{t \geq \tau}$ is a martingale w.r.t. t , with $\exp \ell_{\tau,\tau} = 1$. By Ville's maximal inequality for non-negative supermartingales, we have

$$\mathbb{P}_\infty [\exists t \geq \tau, \exp \ell_{t,\tau} \geq e^b] \leq e^{-b},$$

and for each k ,

$$\mathbb{P}_\infty [\hat{\tau} = t_k^+] \leq e^{-b}.$$

By union bound, for any k ,

$$\mathbb{P}_\infty [\hat{\tau} \geq t_k] = \mathbb{P}_\infty [\hat{\tau} \notin \{t_i^+, i < k\} \cup \{0\}] \geq 1 - \mathbb{P}_\infty [\hat{\tau} = 0] - \sum_{i < k} \mathbb{P}_\infty [\hat{\tau} = t_i^+] \geq 1 - ke^{-b}.$$

$$\mathbb{E}_\infty [|\{k : t_k \leq \hat{\tau}\}|] = \sum_{k=1}^{\lfloor e^b \rfloor} \mathbb{P}_\infty [\hat{\tau} \geq t_k] \geq \sum_{k=1}^{\lfloor e^b \rfloor} (1 - ke^{-b}) \geq \left(\frac{1 - o(1)}{2} \right) e^b.$$

And by the definition of $\hat{\tau}$, there is always $T_C > \hat{\tau}$. Thereby we complete the proof. \square

For i.i.d. observations, the EDD of CUSUM procedure is on the order of $\log(\text{ARL})$ divided by the Kullback–Leibler (KL) divergence for the pre- and post-change distributions. Similar results can be obtained for CUSUM with non-i.i.d. observations (Tartakovsky et al., 2014). We expect a similar result may hold for the CUSUM procedure for Hawkes process, although the complete proof is complicated, which we leave for future research.

Remark 4.2 (EDD of CUSUM). Let

$$I_{KL} = \lim_{t \rightarrow \infty} t^{-1} \ell_{t,0}$$

be the asymptotic KL divergence between the post-change and pre-change processes (since the process the conditional intensity function is stochastic). For any change-point $\kappa \geq 0$ and any event data \mathcal{H}_κ up to κ , we expect the EDD to be

$$\mathbb{E}_\kappa [T_C - \kappa | \mathcal{H}_\kappa] \leq \frac{b}{I_{KL}} (1 + o(1)).$$

Here I_{KL} is irrelevant with κ or \mathcal{H}_κ . We show this for the one-dimensional Hawkes process, where the kernel function φ has finite support and is upper bounded.

$$\begin{aligned}
\mathbb{E}_\kappa [T_c - \kappa | \mathcal{H}_\kappa] &\leq \frac{b}{I_{KL}} + \int_{b/I_{KL}}^\infty \mathbb{P}(T_c - \kappa \geq t) dt \\
&= \frac{b}{I_{KL}} \left(1 + \int_1^\infty \mathbb{P} \left(T_c - \kappa \geq \frac{br}{I_{KL}} \right) dr \right) \\
&\leq \frac{b}{I_{KL}} \left(1 + \int_1^\infty \mathbb{P} \left(\ell_{\kappa+br/I_{KL}, \kappa} \leq b \right) dr \right) \\
&= \frac{b}{I_{KL}} \left(1 + \int_1^\infty \mathbb{P} \left(\frac{I_{KL}}{br} \ell_{\kappa+br/I_{KL}, \kappa} \leq I_{KL}(1 - (r-1)/r) \right) dr \right)
\end{aligned}$$

The concentration bound for $(1/t) \int_0^t f \circ \theta_s ds$ was derived by [Reynaud-Bouret et al. \(2007\)](#), where f is a bounded function on event data during $[-a, 0]$ for some $a > 0$ and θ_s translates the event time by s . They also provide a bound on the number of events in every unit time, which is followed immediately by a bound on the intensity. To be specific, we have $\lambda_0(s), \lambda_\infty(s) \leq O(\log t)$ with probability $1 - O(t^{-c})$ for every $s \in [0, t]$, where c is some large-enough constant. For $\kappa = 0$, the log-likelihood ratio can be written as

$$\begin{aligned}
t^{-1} \ell_{t,0} &= t^{-1} \int_0^t (\lambda_\infty(s) - \lambda_0(s) + \lambda_0(s) \log(\lambda_0(s)/\lambda_\infty(s))) ds \\
&\quad + t^{-1} \int_0^t \log(\lambda_0(s)/\lambda_\infty(s)) (dN_s - \lambda_0(s) ds).
\end{aligned}$$

For the first term, a concentration bound around I_{KL} can be derived using [Reynaud-Bouret et al. \(2007\)](#)'s argument, by first applying the bound on λ_∞ and λ_0 above. We have for any $0 < u \leq O(\sqrt{t})$,

$$\begin{aligned}
\mathbb{P} \left(\left| t^{-1} \int_0^t (\lambda_\infty(s) - \lambda_0(s) + \lambda_0(s) \log(\lambda_0(s)/\lambda_\infty(s))) ds - I_{KL} \right| \geq c_1 \sqrt{\frac{(u + \log t)u}{t}} \log^2 t \right) \\
\leq O(e^{-u}) + O(t^{-c}),
\end{aligned}$$

where c_1 depends on the model and c . The second term is the average of a martingale, and will have a concentration bound around 0 by first applying the bound on $\lambda_\infty, \lambda_0$ and the number of events every unit time, followed by Hoeffding's inequality. We have for any $u > 0$,

$$\mathbb{P} \left(\left| t^{-1} \int_0^t \log(\lambda_0(s)/\lambda_\infty(s)) (dN_s - \lambda_0(s) ds) \right| \geq c_2 u \log^2 t \right) \leq O(e^{-2tu^2}) + O(t^{-c}),$$

where c_2 depends on the model and c . With the two concentration inequality above, we can

check that $\mathbb{E}_0 [T_c | \mathcal{H}_0]$ is $b(1 + o(1))/I_{KL}$. For $\kappa > 0$, since the process restarts at κ , it can be regarded as a translation of the case $\kappa = 0$. The only difference is that λ_∞ takes into consideration the events before κ . Since φ has finite support, such difference only exists for a limited time and will not make a huge difference to the analysis of the EDD.

The KL divergence between different Hawkes models using mean-field approximation is summarized in [Li et al. \(2017\)](#). In particular, the KL divergence for the model shown in (3.1) is given by

$$I_{KL} = (\bar{\boldsymbol{\lambda}}_1)^T (\log \bar{\boldsymbol{\lambda}}_1 - \log \bar{\boldsymbol{\lambda}}_0) - \mathbf{1}^T (\bar{\boldsymbol{\lambda}}_1 - \bar{\boldsymbol{\lambda}}_0),$$

where $\bar{\boldsymbol{\lambda}}_1 = (I_D - A_1)^{-1} \boldsymbol{\mu}$ is the expected intensity for post-change distributions, and $\bar{\boldsymbol{\lambda}}_0 = (I_D - A_0)^{-1} \boldsymbol{\mu}$ is the expected intensity for pre-change distribution. Here I_D is the identity matrix, $\mathbf{1}$ is a vector of ones, $\boldsymbol{\mu} = (\mu_i)_{i \in [D]}$ is the constant base intensity vector, and $A_k = (\alpha_{ij,k})_{i,j \in [D]}, k = 0, 1$. Quantifying the KL-divergence between the pre- and post-change distributions can help us to understand whether a case is easy or difficult to detect.

5 Alternative Detection Procedures

In reality, the post-change parameters are not always known due to the lack of anomaly data. There could be various types of anomalies, and we do not know what to expect. This section considers two other approaches to change-point detection on the Hawkes process: the score and the GLR statistics. Neither of them requires any knowledge regarding the post-change parameters.

5.1 Score Statistics

We consider the score statistics for constructing a detection procedure. The score statistic can detect any deviations from the null hypothesis ([Xie and Siegmund, 2012](#)). It is particularly suitable for detecting small deviation (i.e., locally most efficient) and does not require estimating post-change parameters. The score function is defined as the derivative of the log-likelihood as in (2.6) over the parameters $\alpha_{ij,0}, i, j \in [D]$, on which we would like to detect the change. Let $\boldsymbol{\alpha}_i = (\alpha_{ij})_{j \in [D]} \in \mathbb{R}^{D \times 1}$, the score function on each node i is

$$\frac{\partial \ell_t}{\partial \boldsymbol{\alpha}_i} = - \int_0^t \frac{\partial \lambda_{i,\infty}(s)}{\partial \boldsymbol{\alpha}_i} ds + \int_0^t \lambda_{i,\infty}^{-1}(s) \frac{\partial \lambda_{i,\infty}(s)}{\partial \boldsymbol{\alpha}_i} dN_s^i, \quad (5.1)$$

since $\lambda_{i,\infty}$ only depends on the parameter $\boldsymbol{\alpha}_i$. Then

$$\frac{\partial \ell_t}{\partial \text{vec}(A)} = \left(\frac{\partial \ell_t}{\partial \boldsymbol{\alpha}_1^T}, \dots, \frac{\partial \ell_t}{\partial \boldsymbol{\alpha}_D^T} \right)^T$$

where $A = (\alpha_{ij})_{ij \in [D]}$ and $\text{vec}(A) = (\boldsymbol{\alpha}_1^T, \dots, \boldsymbol{\alpha}_D^T)^T$. In [Ogata (1978), Theorem 3.4], it is shown that the limiting distribution of the score function at the true parameter $A_0 = (\alpha_{ij,0})_{i,j \in [D]}$ is Gaussian

$$\frac{1}{\sqrt{t}} \frac{\partial \ell_t}{\partial \text{vec}(A)} \Big|_{A=A_0} \rightarrow \mathcal{N}(0, I_0),$$

where

$$I_0 = \lim_{t \rightarrow \infty} \frac{1}{t} \mathbb{E} \left[\frac{\partial \ell_t}{\partial \text{vec}(A)} \frac{\partial \ell_t}{\partial \text{vec}^T(A)} \right] \Big|_{A=A_0} = - \lim_{t \rightarrow \infty} \frac{1}{t} \mathbb{E} \left[\frac{\partial^2 \ell_t}{\partial \text{vec}(A) \partial \text{vec}^T(A)} \right] \Big|_{A=A_0},$$

is the Fisher information and is positive definite. Note that the Fisher information is a diagonal block matrix, since for any $i, j, i', j' \in [D]$, $i \neq i'$, $\lambda_{i,\infty}$ is a constant w.r.t. $\alpha_{i',j'}$, and

$$\frac{\partial^2 \ell_t}{\partial \alpha_{i,j} \partial \alpha_{i',j'}} = 0.$$

Each block of I_0 corresponds to $\boldsymbol{\alpha}_i, i \in [D]$, the influence from all nodes to node i . The limiting distribution of the score function at the true parameter can be shown to be

$$\frac{1}{t} \frac{\partial \ell_t}{\partial \text{vec}^T(A)} I_0^{-1} \frac{\partial \ell_t}{\partial \text{vec}(A)} \Big|_{A=A_0} \rightarrow \chi_{D^2}^2.$$

For change-point detection, we adopt the conventional sliding window approach, i.e., calculating the score statistic inside the sliding window $[t-w, t)$ for a suitably chosen window length w , and raise the alarm whenever the statistic exceeds threshold b :

$$T_s = \inf \left\{ t : \frac{1}{w} \frac{\partial(\ell_t - \ell_{t-w})}{\partial \text{vec}^T(A)} I_0^{-1} \frac{\partial(\ell_t - \ell_{t-w})}{\partial \text{vec}(A)} \Big|_{A=A_0} \geq b \right\}.$$

With a sufficiently large window length, the score statistic under the null hypothesis should be around D^2 , the expected value of $\chi_{D^2}^2$ random variable. After the change-point, the expected score function at the pre-change parameters is no longer 0. We would expect the score statistic to be noticeably larger than D^2 , and thus the change is detected.

Like the CUSUM statistics, a memory-efficiency problem arises since the intensity $\lambda_{i,\infty}$ depends on the whole history. We can again replace $\lambda_{i,\infty}$ with $\tilde{\lambda}_{i,\infty}$ using truncated kernels

(similarly, for the GLR statistics in the next subsection). For practical reasons, we also need to choose a grid size γ and only compute the grid's score statistics. We discuss the relation between grid size and EDD for a fixed ARL in Section 6.

5.2 GLR Statistics

When the post-change parameters are unknown, another way to perform change-point detection is to use the generalized likelihood ratio (GLR) statistic. The idea is to find the parameters that best fit the data and compare the likelihood ratio between the fitted parameters and the pre-change ones. The GLR statistic on Hawkes networks was discussed in Li et al. (2017). A sliding window of fixed length w is adopted, and within each window, the log-likelihood ratio is defined as

$$\ell_{t,t-w,\hat{A}} = \sum_{i \in [D]} \int_{t-w}^t \log \left(\frac{\hat{\lambda}_{i,t-w}(s)}{\lambda_{i,\infty}(s)} \right) dN_s^i - \int_{t-w}^t (\hat{\lambda}_{i,t-w}(s) - \lambda_{i,\infty}(s)) ds,$$

where $\hat{\lambda}_{i,t-w}$ is the intensity assuming $t - w$ is the change-point and \hat{A} is the post-change parameter,

$$\hat{\lambda}_{i,t-w}(s) = \mu_i(s) + \sum_{j \in [D]} \hat{\alpha}_{ij} \int_{t-w}^s \varphi_{ij}(s-v) dN_v^j,$$

and $\hat{A} = (\hat{\alpha}_{ij})_{i,j \in [D]}$ is the parameter that maximizes the likelihood in the current window $[t-w, t]$:

$$\hat{A} = \arg \max_{\hat{A}} \sum_{i \in [D]} \int_{t-w}^t \log \lambda_{i,t-w}(s) dN_s^i - \int_{t-w}^t \lambda_{i,t-w}(s) ds.$$

A change is detected when the log-likelihood ratio exceeds certain threshold b :

$$T_G = \inf \{t : \ell_{t,t-w,\hat{A}} \geq b\}.$$

For each window, a convex optimization problem is solved to find the maximum likelihood estimate \hat{A} that best fits the data. However, this operation makes the GLR statistic computationally more expensive than CUSUM and the score statistic. To address this issue, we can use \hat{A} from the previous window as an initialization for the gradient descent algorithm to find the MLE in the next step – this “warm-start” may lead to faster convergence for finding the MLE.

Compared with the score statistic, the GLR statistic is computationally more expensive, and it does not necessarily have better performance (which can be partly due to the noisy MLE estimates), as shown in our example in Section 6. However, the GLR statistic is numer-

ically more stable than the score statistic, especially for large networks. The reason is that we usually may not estimate Fisher information with high accuracy. Even provided with the exact pre-change parameter A_0 , there is no close-form solution for the Fisher information, and it can only be estimated by simulation or real data. The score statistic involves inverting the Fisher information, which can suffer from a high condition number and numerical instability when we try to invert it.

6 Numerical Experiments

In this section, we compare several change-point detection procedures using a simulated example. Consider a small network of $D = 8$ nodes, shown in Figure 3. The background intensity is proportional to the size of the node ranging from 0.5 to 1, and the edges indicate the directed influence between nodes. The edges in black are the pre-change parameters, while the edges in orange show a topological change between nodes 1, 2, and 3. There are two emerging edges after the change-point, with all other edges remain the same.

Figure 4 shows the CUSUM, GLR, and score statistics, respectively, where the dashed line indicates the change-point. As expected, CUSUM grows steadily larger after the change-point. The score and GLR statistics drawn are based on the same sequence of events. They are generally larger after the change-point, while the change in the score statistic is more evident than in the GLR statistic.

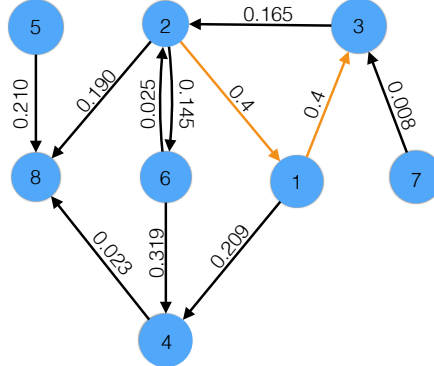


Figure 3: Illustration of the network: Oranges edges emerge after the change-point.

6.1 Performance Comparison

We compare the performance of different statistics by plotting EDD versus $\log(\text{ARL})$ (which is supposed to be close to a straight line according to the theoretical analysis). First, we

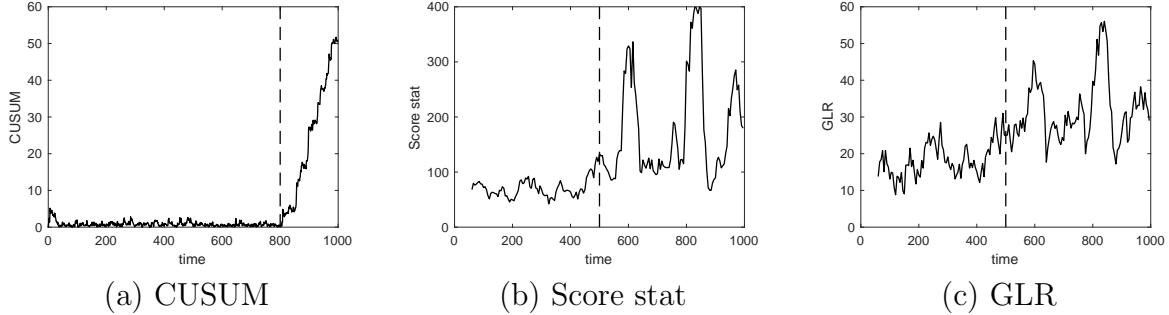


Figure 4: Example of different detecting statistics. Change-point indicated in dash line.

introduce a simple baseline: the Shewhart control chart ([Shewhart, 1925, 1931](#)), which counts the number of events in a sliding window and stops when the number of events falls out of a specific range:

$$T_{\text{Sh}} = \inf\{t : \sum_{i \in [D]} (N_t^i - N_{t-w}^i) \notin [b_1, b_2]\}.$$

This Shewhart chart can detect change in the average intensity. In this example, we only consider the case that the average intensity will be increased after the change-point, and thus choose a one-sided interval by letting $b_1 = 0$.

The comparison results are shown in Figure 5. The CUSUM procedure with exact post-change parameters achieves the best performance, followed by the score statistic and the GLR statistic; all are better than the baseline. For the GLR, score, and Shewhart statistics, we use 60, 60, and 120 as their window lengths, respectively. This corresponds to the optimal window size (found numerically) for an ARL between 500 and 50000. This result shows that the score and GLR statistics use the event data more efficiently than the Shewhart chart, as the Shewhart chart needs a larger window length to identify the difference. Here we set the change-point κ to be slightly larger than the window length w so that for small ARL, the EDD can be smaller than w .

We also consider the CUSUM procedure when the assumed post-change parameter differs from the true one; thus, there is a model mismatch. While the real change happens on two pairs of nodes making the influence factor both 0.4, we consider a CUSUM procedure which assumes a correct post-change network topology; however, the magnitudes of the post-change parameters on the edges are 50% and 200% of the true ones, respectively. We also consider a CUSUM procedure that assumes the correct magnitude of the post-change parameter but an incorrect post-change network topology. In one case, only the change in the influence from $2 \rightarrow 1$ is expected, and in another, a change in the influence from $2 \rightarrow 1, 1 \rightarrow 3, 6 \rightarrow 1, 1 \rightarrow 7$ is expected. The simulation results show that even with misspecified post-change parameters (magnitude or network topology), the CUSUM procedure can still achieve better

performance than the GLR and the score procedures. This demonstrates that the CUSUM procedure is reasonably robust to the misspecification of the post-change parameters.

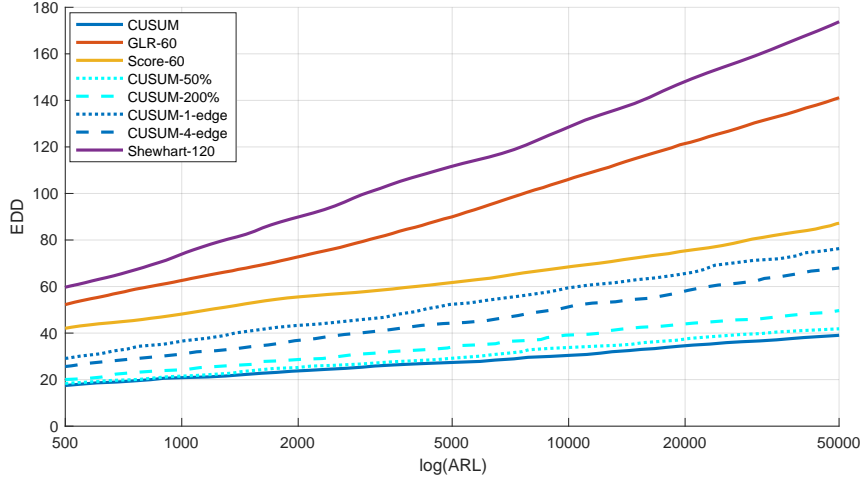


Figure 5: Performance comparison between different statistics. The window length of the GLR, score statistics and Shewhart chart is chosen to be 60, 60, and 120 respectively. For the CUSUM statistic, we also test its performance when either the scale (50% and 200% of the real one) or the topology (one edge $2 \rightarrow 1$ and four edges $2 \rightarrow 1, 1 \rightarrow 3, 6 \rightarrow 1, 1 \rightarrow 7$) of the change is not correctly estimated.

6.2 Effect of Grid Size γ

The choice of the grid size γ involves a trade-off between algorithm performance and complexity. In this example, we compare CUSUM, the GLR, and the score statistics with a grid size γ ranging from 0.1 to 50. For the EDD, we assume that the change-point is uniformly distributed between two grid points. Figure 6 shows the effect of the grid size on CUSUM, the GLR, and the score procedure. We find that a large grid size γ will result in both larger ARL and EDD, and if we tune the threshold b to fix the ARL, the EDD may still increase with a larger γ .

To understand the effect of γ on computation complexity, we mainly consider the GLR statistic as the computation for the GLR is the most expensive. To solve the convex optimization problem for each window, we use the EM algorithm as described in [Li et al. \(2017\)](#) and terminate when the update in the log-likelihood is less than 10^{-4} . Figure 6(c) shows the average iterations needed per window for different grid sizes.

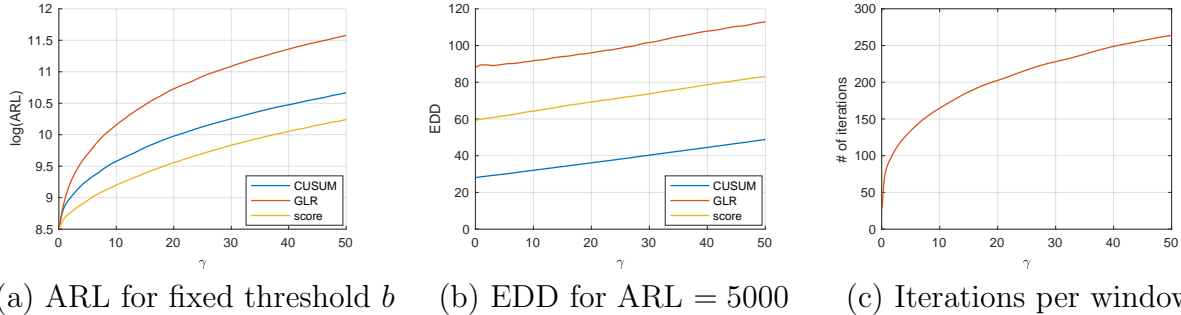


Figure 6: Effect of the grid size γ on CUSUM, GLR, and score statistics. The window length for the GLR and the score statistics is 60 and for Shewhart is 120, which are optimized for better EDD performance. (a) shows the effect of γ on the ARL. The threshold b for CUSUM, the GLR and the score statistics are 6.319, 37.66, and 148.2 respectively, making ARL = 5000 at $\gamma = 0.1$. (b) shows the effect of γ on the performance of the three statistics. Here the threshold b is tuned so that the ARL is 5000. (c) shows the average number of iterations per window needed in the GLR statistic for the optimization problem to converge.

7 Detecting Neuronal Network Population Code Change

We now return to the motivating problem of detecting population code changes in neuronal networks. The data considered are neural spike trains, which record the sequence of times when a neuron fires an action potential. The multivariate Hawkes processes from Section 2.2 have been used for modeling spike train data (Lambert et al., 2018; Wang et al., 2020b), and capture two appealing features for neuronal networks. First, the base intensities μ_i capture noisy influences on neuron i , resulting from either unobserved neurons or external stimuli. Second, the influence parameters α_{ij} capture the functional influence from neuron j to neuron i due to electrochemical dynamics.

We are interested in detecting the change-point in the underlying population code in neural data. These are *abrupt* changes, as the behavior of populations of neurons respond quickly (usually in just a few ms) to changing input. Population codes are a distributed representation of information used widely across many neural architectures and have been most widely documented in the cortex. As opposed to dense representations, population codes consist of sparsely activated subsets of neurons in which the information is distributed amongst the entire subset. Figure 7 illustrates this idea. The left plots show a plausible neuronal network topology for the population coding of seeing a cat or a dog. The right plots show the corresponding spike train data on the neuronal network, as one changes states from a cat to a dog. Identifying this population code change-point from experimental data allows scientists to better understand the role of each neuron in the network and the corresponding relationship between stimulus and response.

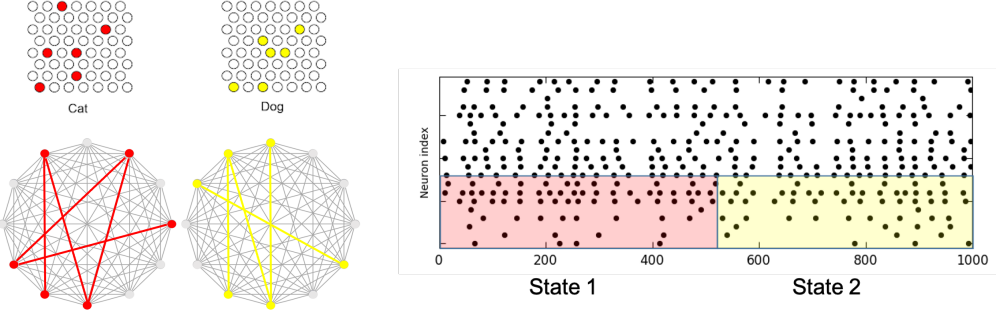


Figure 7: (Left) A plausible network topology for ‘Cat’ and ‘Dog’; (Right) Spike train data for each neuron under a population code change.

While there have been significant advances in neuroimaging technology, it can still be quite expensive to record fine-scale spiking data through in-vivo experiments. To illustrate the proposed method, we instead simulate the spike trains using the PyNN package with the NEURON simulator, which implements the neuronal model in [Brette and Gerstner \(2005\)](#). We build off previous work in neural simulation and use a network of exponential integrate-and-fire neurons with spike triggered and sub-threshold adaptation currents.

The simulation set-up is as follows. We first simulate several small networks of neurons in a balance of 80-20 excitatory to inhibitory neurons, with network size fixed at $D = 14$ neurons. From this, we obtain a continuous readout of each neuron spiking data. Each neuron then receives a small Gaussian noise current, representing random external influence on the network. In addition, a select few neurons receive inputs from an external source, which represents the phenomenon of sparse population coding. The neurons that spike at higher rates form a distributed representation of the network state.

We then randomly selected two such subsets of neurons, representing two different states. We simulate the network in the first state for a long time (from $t = 0$ - 20,000 ms) to learn network dynamics and structure under the first population code. The pre-change Hawkes process parameters are obtained via maximum likelihood estimation (MLE) on the pre-change spike train data. After $\kappa = 20,000$ ms, we then simulate a change from the first to the second state. The goal is to quickly detect the change-point κ in a sequential fashion from the simulated spike trains. For CUSUM, the post-change Hawkes process parameters are estimated via MLE on the post-change spike trains. For the score statistic, the pre-change Fisher information matrix I_0 is highly ill-conditioned when estimated from spike trains, so we instead use a slightly regularized estimate $I_0 + \lambda I$, where $\lambda = 1$ and I is an identity matrix. The estimated pre-change and post-change models are shown in Figure 8.

Figure 9 shows the CUSUM, GLR, and score statistics, respectively, with the dashed line indicating the change-point in population code. Both the score and GLR statistics utilize

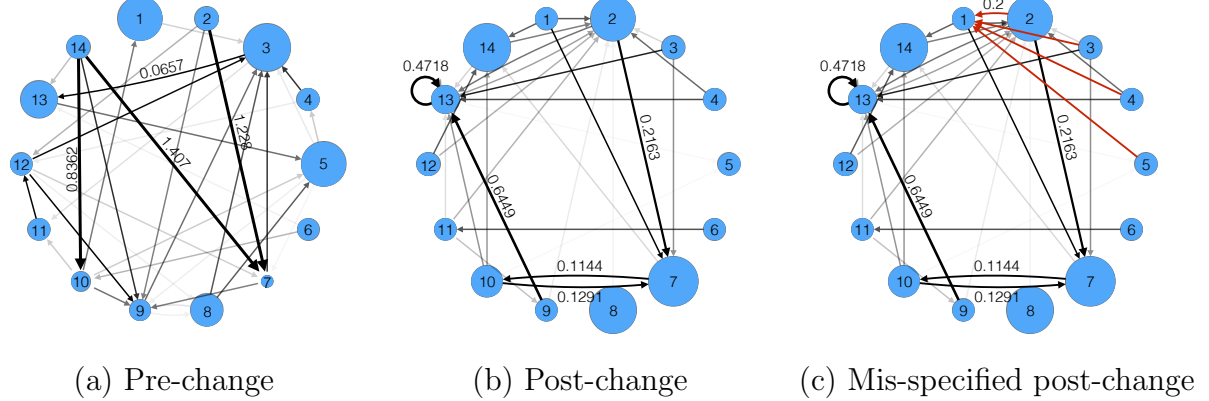


Figure 8: (a)(b) shows the estimated pre-change and post-change parameters. The size of the nodes are proportional to their background intensities ranging from 0 to 0.016. The opacity of the unlabeled edges are proportional to their weights, ranging from 0 to 0.06. (c) shows a case of post-change topology misspecification in CUSUM statistic.

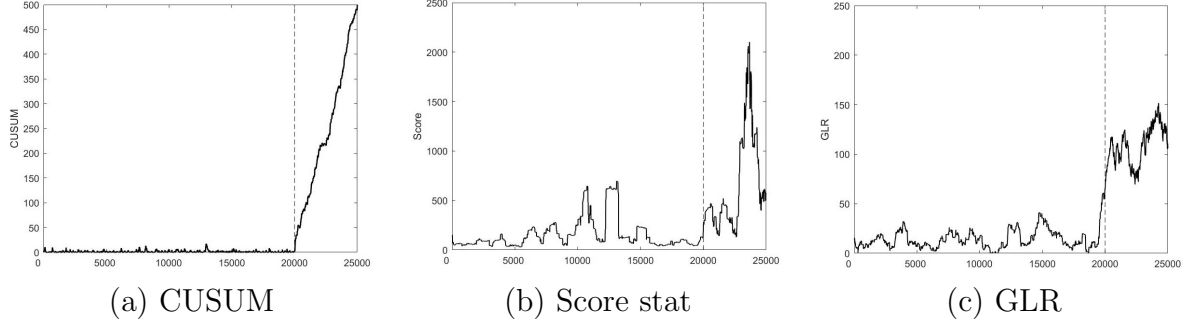


Figure 9: Example of different detecting statistics for the neuronal network application. Change-point indicated in dash line.

a window size of 1,000 and an update rate of $\gamma = 5$. As in numerical experiments, we see that the CUSUM statistic increases rapidly after the change-point, which shows it is quite effective at detecting the underlying neuronal network changes. The score and GLR statistics are also noticeably larger after the change-point, with the increase in GLR more prominent than the increase for the score statistic. The increase in GLR and score is noticeably lower than that for the proposed CUSUM procedure, which suggests that our method can better detect population code changes in neuronal networks.

Next, we consider the case where post-change parameter estimates are misspecified for the CUSUM statistic. This may arise, e.g., when there is a lack of spike train data for post-change parameter estimation. We consider three scenarios for misspecification: (a) the post-change topology is correct, but the influence parameters are scaled at 200%, (b) the influence parameters are correct, but there are spurious edges on neuron 1 for the topology (see Figure 10(b)), (c) the post-change influence parameters are correct, but all the edges to

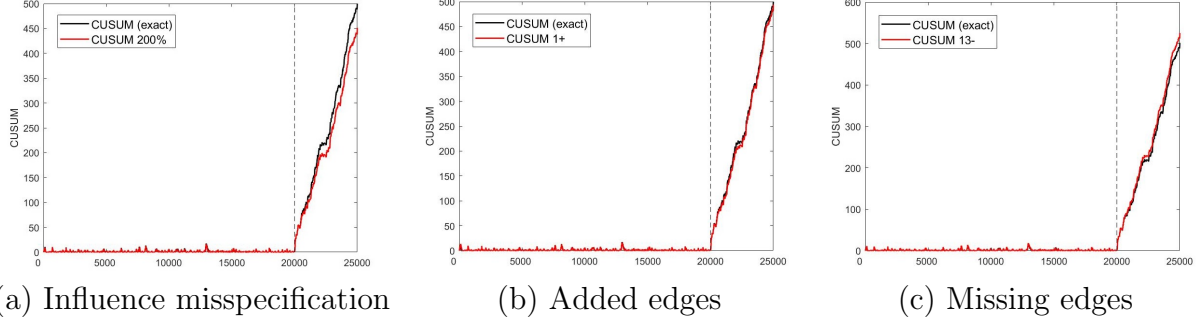


Figure 10: CUSUM statistics under different misspecifications of post-change parameters. The red line shows the CUSUM statistic under an “exact” specification of post-change parameters, and the dash line indicates the change-point.

neuron 13 are missing for the topology. Figure 10 shows the CUSUM statistics for these three scenarios, along with the “exact” CUSUM statistics, which use exact post-change MLEs. We see that the CUSUM is quite robust: its CUSUM statistics are quite close to the exact CUSUM for both influence and topology misspecifications. Hence, our method appears to efficiently detect population code changes, even under uncertainties in post-change parameter estimation.

8 Conclusion and Discussions

We have presented a new sequential CUSUM procedure for detecting change-point in the multi-dimensional self- and mutual-exciting point processes, a.k.a. the Hawkes processes. By tackling the complex and long-term dependence between event times, we develop the CUSUM procedure that enjoys efficient recursive computation and memory efficiency if we employ truncation. Using numerical experiments, we found that the CUSUM performs better than other detection procedures (Shewhart type) based on score statistics and generalized likelihood ratio (GLR) statistics from the existing literature. Moreover, we found that although the CUSUM procedure requires specifying the post-change distribution parameters, it is fairly robust to parameter misspecification and still outperforms other methods. This can be partly explained by that the alternative methods are the Shewhart type, based on evaluating a detection statistic using the sliding window, which does not accumulate information from the past and, in our case, requires a fairly additional estimation of the post-change parameters. We also demonstrated the potential application of our procedure for neuronal network change-point detection.

Funding

The work of Haoyun Wang, Liyan Xie, and Yao Xie is supported by the NSF CAREER Award CCF-1650913, and NSF CMMI-2015787, DMS-1938106, DMS-1830210. Simon Mak is supported by NSF CSSI Frameworks grant 2004571.

REFERENCES

Brette, R. and Gerstner, W. (2005). Adaptive Exponential Integrate-and-Fire Model as an Effective Description of Neuronal Activity, *Journal of Neurophysiology* 94: 3637–3642.

Daley, D. J. and Vere-Jones, D. (2003). *An Introduction to the Theory of Point Processes: Volume I: Elementary Theory and Methods*, New York: Springer.

Hawkes, A. G. (1971). Spectra of Some Self-Exciting and Mutually Exciting Point Processes, *Biometrika* 58: 83–90.

Hawkes, A. G. (2018). Hawkes Processes and Their Applications to Finance: A Review, *Quantitative Finance* 18: 193–198.

Lambert, R. C., Tuleau-Malot, C., Bessaih, T., Rivoirard, V., Bouret, Y., Leresche, N., and Reynaud-Bouret, P. (2018). Reconstructing the Functional Connectivity of Multiple Spike Trains Using Hawkes Models, *Journal of Neuroscience Methods* 297: 9–21.

Li, S., Xie, Y., Farajtabar, M., Verma, A., and Song, L. (2017). Detecting Changes in Dynamic Events over Networks, *IEEE Transactions on Signal and Information Processing over Networks* 3: 346–359.

Lorden, G. (1971). Procedures for Reacting to a Change in Distribution, *Annals of Mathematical Statistics* 42: 1897–1908.

Mohler, G. O., Short, M. B., Brantingham, P. J., Schoenberg, F. P., and Tita, G. E. (2011). Self-Exciting Point Process Modeling of Crime, *Journal of the American Statistical Association* 106: 100–108.

Ogata, Y. (1978). The Asymptotic Behaviour of Maximum Likelihood Estimators for Stationary Point Processes, *Annals of the Institute of Statistical Mathematics* 30: 243–261.

Ogata, Y. (1988). Statistical Models for Earthquake Occurrences and Residual Analysis for Point Processes, *Journal of the American Statistical association* 83: 9–27.

Ogata, Y. (1998). Space-Time Point-Process Models for Earthquake Occurrences, *Annals of the Institute of Statistical Mathematics* 50: 379–402.

Page, E. S. (1954). Continuous Inspection Schemes, *Biometrika* 41: 100–115.

Pollak, M. (1985). Optimal Detection of a Change in Distribution, *Annals of Statistics* 13: 206–227.

Rambaldi, M., Filimonov, V., and Lillo, F. (2018). Detection of Intensity Bursts Using Hawkes Processes: An Application to High-Frequency Financial Data, *Physical Review E* 97: 032318.

Rasmussen, J. G. (2011). *Temporal Point Processes: The Conditional Intensity Function*, Lecture Notes, Jan.

Reinhart, A. (2018). A Review of Self-Exciting Spatio-Temporal Point Processes and Their Applications, *Statistical Science* 33: 299–318.

Reynaud-Bouret, P., Rivoirard, V., and Tuleau-Malot, C. (2013), Inference of Functional Connectivity in Neurosciences via Hawkes Processes, in *Proceedings of IEEE Global Conference on Signal and Information Processing*, pp. 317–320.

Reynaud-Bouret, P. and Roy, E. (2007). Some Non-Asymptotic Tail Estimates for Hawkes Processes, *Bulletin of the Belgian Mathematical Society-Simon Stevin* 13: 883–896.

Rizoiu, M. A., Mishra, S., Kong, Q., Carman, M., and Xie, L. (2018). SIR-Hawkes: Linking Epidemic Models and Hawkes Processes to Model Diffusions in Finite Populations, in *Proceedings of World Wide Web Conference*, pp. 419–428.

Shewhart, W. A. (1925). The Application of Statistics as an Aid in Maintaining Quality of a Manufactured Product, *Journal of the American Statistical Association* 20: 546–548.

Shewhart, W. A. (1931). *Economic Control of Quality of Manufactured Product*, London: Macmillan And Co. Ltd.

Tang, S., Zhang, Y., Li, Z., Li, M., Liu, F., Jiang, H., and Lee, T. S. (2018). Large-Scale Two-Photon Imaging Revealed Super-Sparse Population Codes in the V1 Superficial Layer of Awake Monkeys, *Elife* 7: e33370.

Tartakovsky, A., Nikiforov, I., and Basseville, M. (2014), *Sequential Analysis: Hypothesis Testing and Changepoint Detection*, New York: CRC Press.

Wang, D., Yu, Y., and Willett, R. (2020a). Detecting Abrupt Changes in High-Dimensional Self-Exciting Poisson Processes, *arXiv preprint arXiv:2006.03572*.

Wang, H., Xie, L., Cuozzo, A., Mak, S., and Xie, Y. (2020b). Uncertainty Quantification for Inferring Hawkes Networks, in *Proceedings of Advances in Neural Information Processing Systems*.

Xie, L., Xie, Y., and Moustakides, G. V. (2020). Sequential Subspace Change Point Detection, *Sequential Analysis*, 39: 307–335.

Xie, L., Zou, S., Xie, Y., and Veeravalli, V. V. (2021). Sequential Change Detection: Classical Results and New Directions, *IEEE Journal on Selected Areas in Information Theory*.

Xie, Y. and Siegmund, D. (2012). Spectrum Opportunity Detection with Weak and Correlated Signals, in *Proceedings of Forty Sixth Asilomar Conference on Signals, Systems and Computers (ASILOMAR)*, pp. 128–132.

Yang, S. H. and Zha, H. (2013). Mixture of Mutually Exciting Processes for Viral Diffusion, in *Proceedings of International Conference on Machine Learning*, pp. 1–9.

Zhou, F., Li, Z., Fan, X., Wang, Y., Sowmya, A., and Chen, F. (2020). Fast Multi-Resolution Segmentation for Nonstationary Hawkes Process using Cumulants, *International Journal of Data Science and Analytics* 10: 321–330.